Three-Dimensional, T1-Weighted Gradient-Echo Imaging of the Brain with a Volumetric Interpolated Examination

Stephan G. Wetzel, Glyn Johnson, Andrew G. S. Tan, Soonmee Cha, Edmond A. Knopp, Vivian S. Lee, David Thomasson and Neil M. Rofsky

AJNR Am J Neuroradiol 2002, 23 (6) 995-1002
http://www.ajnr.org/content/23/6/995

AJNR Am J Neuroradiol 23:995–1002, June/July 2002

Three-Dimensional, T1-Weighted Gradient-Echo Imaging of the Brain with a Volumetric Interpolated Examination

Stephan G. Wetzel, Glyn Johnson, Andrew G. S. Tan, Soonmee Cha, Edmond A. Knopp, Vivian S. Lee, David Thomasson, and Neil M. Rofsky

BACKGROUND AND PURPOSE: **T1-weighted, 3D gradient-echo MR sequences can be optimized for rapid acquisition and improved resolution through asymmetric k-space sampling and interpolation. We compared a volumetric interpolated brain examination (VIBE) sequence with a magnetization-prepared rapid acquisition gradient echo (MP RAGE) sequence and a 2D T1-weighted spin-echo (SE) sequence.**

METHODS: **Thirty consecutive patients known or suspected to have focal brain lesions underwent postcontrast studies (20 mL of gadopentetate dimeglumine) with VIBE, MP RAGE, and 2D T1-weighted SE imaging. Source and 5-mm VIBE and MP RAGE reformations, and 5-mm T1-weighted SE images were compared qualitatively and by using signal-to-noise ratio (SNR) and contrast-to-noise ratio (CNR). SNRs in a gadolinium-doped water phantom were also measured for all three sequences.**

RESULTS: **On the source images, SNRs for gray matter (GM) and white matter (WM), and CNRs for WM-to-GM and contrast-enhancing lesion-to-GM were slightly, but significantly higher for the VIBE sequence than for the MP RAGE sequence ($P < .05$). On 5-mm reformations, WM-to-GM CNR was significantly higher on VIBE and MP RAGE images than on T1-weighted SE images ($P < .001$), but contrast-enhancing lesion-to-GM CNRs were higher on SE images compared with both gradient-echo sequences ($P < .001$). Qualitatively, VIBE images showed fewer flow artifacts than did SE and MP RAGE images ($P < .05$). In the phantom, VIBE SNR was higher than MP RAGE SNR for short T1 relaxation times.**

CONCLUSION: **VIBE provides an effective, alternative approach to MP RAGE for fast 3D T1-weighted imaging of the brain.**

Gradient-echo (GRE) MR sequences allow the acquisition of T1-weighted 3D data sets of the brain that can be reformatted to provide images in different orientations, a process often called multiplanar reconstruction (1, 2). For effective multiplanar reconstruction in brain imaging, images must be obtained with approximately isotropic resolution and a small voxel volume (typically <2 mm^3). Sequences with ultrashort TR (eg, $\leq$10 msec) are capable of generating such high-spatial-resolution data sets in a reasonable time frame for clinical use.

To date, the most widely used T1-weighted 3D GRE sequence is a magnetization-prepared rapid acquisition GRE (MP RAGE) sequence that incorporates an MP inversion pulse to increase T1 weighting (3, 4). With appropriate timing parameters, these sequences can give excellent contrast, such as between gray matter (GM) and white matter (WM). However, both theoretic (5) and clinical studies (4, 6–8) have demonstrated that contrast material–enhancing lesions might be less conspicuous and can be missed on MP RAGE images, compared with T1-weighted spin-echo (SE) images.

Rofsky et al (9) described an interpolated 3D T1-weighted GRE sequence referred to as volumetric interpolated *breath-hold* examination for abdominal imaging. This commercially available sequence is optimized for short acquisition times and achieves resolution improvements through the use of asymmetric

Received April 16, 2001; accepted after revision March 4, 2002.

From the Department of Radiology, New York University Medical Center, NY (S.G.W, G.J., A.G.S.T., S.C., E.A.K., V.S.L.); Siemens Medical Systems, Washington, DC (D.T.); and Magnetic Resonance Imaging, Beth Israel Deaconess Medical Center, Harvard Medical School, Boston, MA (N.M.R.).

S.G.W. supported by Swiss National Science Foundation/Karger Stiftung and by Novartis Stiftung.

Presented in part at the 39th annual meeting of the American Society of Neuroradiology, Boston, April 2001.

Address reprint requests to Glyn Johnson, PhD, Department of Radiology (Research), New York University School of Medicine, 550 First Ave, New York, NY 10016.

k-space sampling and interpolation. This type of sequence can also be used to form rapid, high-spatial-resolution images of the brain. Furthermore, it is a very efficient sequence because data collection is continuous, whereas approximately half of the MP RAGE imaging time is required for preparation and recovery periods. We hypothesized that a volumetric interpolated brain examination (VIBE) sequence may serve as an efficient alternative to MP RAGE for acquiring high-spatial-resolution, high-contrast T1-weighted brain images.

The goal of our study was to compare VIBE imaging with MP RAGE and 2D T1-weighted SE imaging in both a phantom and patients.

Methods

MR imaging was performed with a 1.5-T system (Vision; Siemens Medical Systems, Iselin, NJ) with maximum gradient strength of 25 mT/m and rise time of 600 μs, with use of a quadrature head coil.

MR Sequences and Parameters

The following nomenclature describes encoding directions: "phase-encoding direction" refers to the in-plane phase-encoding direction, and "partition-encoding direction" refers to the through-slab phase-encoding direction.

VIBE.—The VIBE sequence is a radio-frequency–spoiled 3D GRE sequence (8.8/4.4 [TR/TE], 15° flip angle). The data were acquired sagittally with a field of view of 210 × 210 mm or 220 × 220 mm, and the slab thickness was 160 mm. The data matrix was 256 (read) × 192 (phase) × 108 (partition). Sampling was symmetric in the read and phase-encoding directions giving an in-plane resolution of 0.82 × 1.09 mm. In the partition direction, the center of k space fell at line 32/108. Before Fourier transformation, the partition direction was zero-filled to 216 points. Other parameters were number of signal averages, 2; bandwidth, 195 Hz per pixel; and acquisition time, 6 minutes.

The flip angle was calculated to maximize contrast by using the following equation derived by Buxton et al (10):

$$\alpha = \cos^{-1}\left[\frac{2\exp(-\mathrm{TR}/\mathrm{T1}) - 1}{2 - \exp(-\mathrm{TR}/\mathrm{T1})}\right],$$

where T1 = 800 ms. This equation gives the flip angle that optimizes contrast in spoiled T1-weighted GRE sequences for small changes in T1. Comparison of WM-to-GM contrast-to-noise ratio (CNR) in five healthy volunteers at a variety of flip angles close to this value confirmed that the contrast was near optimum.

MP RAGE.—For this sequence, we used the following parameters: 9.7/4.0/300 [TR/TE/TI], 15° flip angle; time between consecutive inversions, 2462 ms; one acquisition. These parameters were based on those recommended by our system's manufacturer but optimized at our institution over the course of 7 years of use. Other groups have used similar parameters (7, 8, 11, 12). These data also were acquired sagittally with field-of-view, slab thickness, and data matrix identical to those of the VIBE sequence, in the same acquisition time of 6 minutes. However, sampling was symmetric in all dimensions, giving voxel dimensions of 0.82 × 1.09 × 1.25 mm (128 partitions). Note that although VIBE and MP RAGE provide a similar spatial resolution, the relative efficiency of VIBE allows two signals to be acquired in approximately the same imaging time.

Two-Dimensional T1-Weighted SE.—The following parameters were used: 600/14, 65° flip angle; field-of-view, 200–220 mm; data acquisition matrix, 192 (phase) × 256 (read). Twenty sections with thickness of 5 mm and an intersection gap of 1.5 mm were acquired in the (para)axial plane with one acquisition. Two signals were averaged for an acquisition time of 3 minutes.

Phantom Study

The phantom consisted of an array of 16 plastic tubes filled with distilled water doped with graded concentrations of gadopentetate dimeglumine (Magnevist; Berlex, Wayne, NJ). Contrast material concentration was calculated to give a range of T1 values between 5 and 2600 ms, using relaxivity data provided by the manufacturer, and checked empirically by calculating T1 values from a series of inversion-recovery images. Phantom images were obtained with the VIBE, MP RAGE, and 2D T1-weighted SE sequences. Imaging parameters were identical to those used for the clinical evaluation, as described above. Signal-to-noise ratios (SNRs) for each T1 value were determined by measuring signal intensity in a region-of-interest (ROI) within each bottle and the standard deviation of the noise in an ROI in air. SNRs for VIBE and MP RAGE images were evaluated for the 5-mm reformations.

Patients and Protocol

Thirty consecutive patients (15 women, 15 men; mean age, 55.4 years; age range, 18–80 years) examined over a 6-week interval between June and August 2000 were included in this study. Patient inclusion criterion was a clinically indicated contrast-enhanced MR imaging examination of the brain for suspicion of a focal brain lesion on the basis of previous CT and/or conventional MR imaging or clinical suspicion of such a lesion. Outpatients and patients receiving a triple dose of contrast agent who underwent perfusion MR imaging or MR spectroscopy or who could not undergo extended imaging due to severe claustrophobia or discomfort were excluded. Clinical indications for MR imaging were postoperative follow-up after brain surgery in 19 patients (high-grade gliomas [n = 9], metastatic disease [n = 3], meningeomas [n = 3], others [n = 4]), suspicion of metastatic disease or CNS lymhoma in 10 patients, and multiple sclerosis in one patient. Approval for these studies was obtained from the Board of Research Associates, and informed consent was obtained from all patients.

The 2D T1-weighted SE images, MP RAGE images, and VIBE images were obtained after slow intravenous administration (manual injection) of 20 mL of gadopentetate dimeglumine. The order of the postcontrast T1-weighted imaging sequences was randomized to avoid bias caused by changing concentrations of gadopentetate dimeglumine with time after injection. The delay time between contrast material administration and the start of the first investigated T1-weighted sequence was between 5 and 10 minutes in all patients. In all patients, axial precontrast T1-weighted SE images, axial T2-weighted turbo-SE images, and fluid-attenuated inversion recovery (FLAIR) images were acquired as part of the routine imaging protocol.

Image Processing

The VIBE and MP RAGE images were postprocessed on the manufacturers satellite workstation by one investigator (S.G.W.) who was not involved with the qualitative comparison. Data were reformatted into 5-mm-thick sections with an interval of 1.5 mm in the para(axial) plane to match the locations of the 2D T1-weighted SE images. A total of five postcontrast image sets were assessed: T1-weighted SE images, 5-mm MP RAGE reformations, 5-mm VIBE reformations, MP RAGE source images, and VIBE source images.

Quantitative Assessment of Image Quality

ROI analysis was performed on all (para)axial postcontrast 2D T1-weighted SE images, VIBE and MP RAGE reformations, and VIBE and MP RAGE source images by a single investigator (A.G.S.T.). ROIs were placed over the GM (measured in the head of the caudate nucleus) and WM (measured in the genu of the corpus callosum). Noise was measured as standard deviation, δ, of signal intensity defined by an ROI measured in air. SNRs were measured in ROIs in all enhancing lesions with a diameter of at least 5 mm. When two or more contrast-enhancing regions were seen within the same confluent region of signal hyperintensity on T2-weighted images, only the largest region was evaluated. All SNR measurements were made on two separate occasions and averaged. Placement and cursor size of ROIs were matched for the different image sets in a given patient.

GM and WM SNRs were calculated as SI_{GM}/δ and SI_{WM}/δ, respectively, where SI is signal intensity. WM–GM, lesion–GM, and lesion–WM CNR values were calculated as $(SI_{WM} - SI_{GM})/\delta$, $(SI_{lesion} - SI_{GM})/\delta$, and $(SI_{lesion} - SI_{WM})/\delta$, respectively.

Qualitative Assessment of Image Quality

Two independent, experienced neuroradiologists (S.C., E.A.K.), blinded to patient information and sequence type, viewed sets of 20 postcontrast images in random order. Each set consisted of the 20 images obtained with a single sequence and displayed on a single sheet of film. There were three sets (T1-weighted SE images, 5-mm VIBE reformations, and 5-mm MP RAGE reformations) per patient for a total of 60 images. The three image sets of a given patient were presented in random order at three reading sessions. To avoid recall biasing of the observers, the different reading sessions were separated by an interval of at least 2 weeks.

The number and location of hyperintense lesions was recorded. Because only postcontrast images were given to the readers, hyperintense lesions represented either contrast-enhancing lesions or primarily hyperintense lesions (eg, areas of subacute bleeding). The following three types of artifact were also assessed: motion-induced, flow-related, and ringing artifacts. All artifacts were assessed with the following five-point scale: 1, unreadable, nondiagnostic study; 2, severe artifacts, but diagnostic study; 3, moderate artifacts; 4, mild artifacts; 5, not encountered. The location of circumscribed artifacts was recorded.

After the first reading, a second reading session was held in which all three image sets of a given patient were presented together. The same readers were still blinded to the imaging sequence and independent. The three imaging techniques were rated for conspicuity of hyperintense lesions by using a forced choice method as 1, best; 2, intermediate; and 3, worst.

Finally, a consensus reading was performed by the two neuroradiologists, at which time each patient's T1-weighted, FLAIR, and turbo SE T2-weighted images as well as clinical information were available. At the consensus reading, the number and location of enhancing lesions was determined to form a standard of reference. Lesions that were hyperintense on precontrast T1-weighted SE images, but that did not enhance, were determined separately and attributed to the most likely pathology. At this point, the VIBE and MP RAGE source images were also assessed.

Statistical Analysis

Quantitative.—SNRs and CNRs were compared for the MP RAGE and VIBE source images by means of a paired, two-tailed Student *t* test. To compare the 5-mm MP RAGE reformations, 5-mm VIBE reformations, and 2D T1-weighted SE images for the same parameters, an analysis of variance test was used, taking into account the correlation between the three samples (within-subjects analysis of variance, SPSS 9.0; SPSS, Chicago, IL). For those parameters for which a statistically significant difference was observed ($P < .05$), a paired, two-tailed Student *t* test was applied.

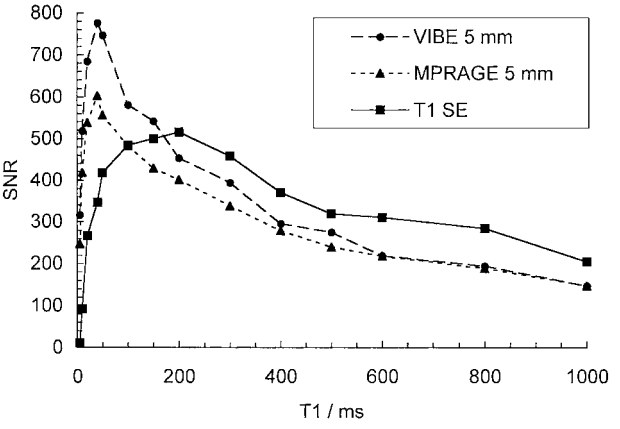

FIG 1. SNR measurements obtained on a phantom for T1 values between 5 and 1000 ms for the 5-mm VIBE and MP RAGE reformations and the T1-weighted SE images.

Qualitiative.—The Friedman nonparametric test for related samples was used to compare differences in the subjective ratings of image quality and subjective ranking of lesion conspicuity among the three sequences. With parameters for which a statistically significant difference in ratings was observed, a comparison between pairs of techniques was made by means of the Wilcoxon signed rank test. The interobserver concordance for ranking of lesion conspicuity was assessed with a κ correlation test. The interobserver concordance for ratings of image quality was expressed as the percentage of agreement between the two readers. This was necessary because the data did not fulfill the requirements for κ statistics (reader one chose scoring categories not applied by reader two).

Results

Phantom Study

Phantom SNRs measured with T1-weighted SE, MP RAGE, and VIBE sequences for T1 values up to 1000 ms are plotted in Figure 1. Up to T1 values of 200 ms, SNRs increase monotonically with decreasing T1. In general, T1-weighted SE SNR values were the largest, followed by VIBE and then MP RAGE, although for T1 values longer than 600 ms, differences between the two GRE sequences were negligible. T1-weighted SE SNRs decline for T1 values below 200 ms, but VIBE and MP RAGE values continue to increase to T1 of about 50 ms. VIBE SNRs were considerably higher than MP RAGE values at these short T1 times.

Patient Studies

Quantitative Analysis.—ROI analysis of 16 contrast-enhancing lesions was performed in 12 patients. Mean SNR and CNR values are listed in Table 1. SNRs for GM and WM, GM-WM CNRs, and contrast-enhancing lesions–GM CNRs were significantly higher on the VIBE source images than on the MP RAGE source images ($P < .05$). On the 5-mm VIBE reformations, the lesion-GM CNR was significantly higher than that on the 5-mm MP RAGE reforma-

TABLE 1: Summary of SNR and CNR Results

Images	SNR		CNR		
	GM	WM	GM-WM	Lesion-GM	Lesion-WM
Source					
MP Rage	23.1 ± 5.2	27.8 ± 5.0	4.8 ± 1.5	16.3 ± 10.2	11.8 ± 10.3
VIBE	26.1 ± 5.4	32.0 ± 6.3	5.9 ± 2.2	20.2 ± 11.3	14.3 ± 12.0
P value	.001	<.001	<.001	.002	.053
5-mm Reformations					
MP RAGE	73.8 ± 14.6	89.2 ± 15.1	15.4 ± 4.1	38.9 ± 26.3	25.1 ± 26.1
VIBE	77.5 ± 14.5	94.2 ± 16.3	16.8 ± 4.4	46.1 ± 26.4	30.0 ± 28.3
T1-weighted SE	96.1 ± 11.0	106.4 ± 10.1	10.2 ± 4.9	64.1 ± 37.9	54.1 ± 39.1
P value*	<.001†	<.001†	<.001†	<.001‡	<.001†

Note.—Data are mean ratios ± SD.

* *P* values are based on analysis of variance.

† Paired Student *t* test demonstrated no significant difference between 5-mm VIBE and MP RAGE reformations.

‡ Student *t* test demonstrated a statistically significant difference between each pairing of images obtained with the three imaging methods.

TABLE 2: Subjective artifact assessment

Artifact	T1-Weighted SE Images	VIBE 5-mm Reformations	MP RAGE 5-mm Reformations	*P* Value*
Gross patient motion	5.00 ± 0.0	4.98 ± 0.1	4.92 ± 0.2	0.039
Flow-related	3.73 ± 0.4	4.33 ± 0.6	4.02 ± 0.6	<0.001†
Ringing (truncation)	4.25 ± 0.4	3.92 ± 0.4	3.83 ± 0.6	<0.001‡

Note.—Data are mean grade ± SD. Grading scheme: 1, unreadable, nondiagnostic study; 2, severe artifacts, but diagnostic study; 3, moderate artifacts; 4, mild artifacts; 5, not encountered.

* *P* values are based on analysis of variance.

† Wilcoxon signed rank test demonstrated a statistically significant difference between each pairing of images obtained with the three imaging methods.

‡ The Friedman nonparametric test showed significant differences between the three sequences considered together. However, the difference between MP RAGE and VIBE was not significant on the Wilcoxan signed rank sum test.

tions. GM-WM CNRs were significantly higher on both the 5-mm MP RAGE and VIBE reformations than on T1-weighted SE images. However, WM SNR, GM SNR, lesion-GM CNR, and lesion-WM CNR were significantly higher on T1-weighted SE images.

Image Quality, Lesion Detection, and Lesion Conspicuity.—Table 2 summarizes the mean scores for image artifacts. In 99.3% of all ratings for image quality, the two observers differed by no more than one category on the scaling scheme. In 72.2%, the ratings were identical, indicating a good interobserver agreement. Among the artifacts encountered, both GRE sequences were more prone to ringing (truncation) artifacts than was the T1-weighted SE sequence. However, flow-related artifacts were more prominent on T1-weighted SE images than on images with both GRE sequences. Flow artifacts on the T1-weighted SE images were all found in the posterior fossa and were due to pulsatile flow in the venous sinuses. Similar artifacts, either from the internal carotid artery or the venous sinuses, were found on MP RAGE images of the posterior fossa, impairing evaluation of the pons in particular (Fig 2). These artifacts were also encountered with the VIBE sequence, but to a statistically significant lower degree.

At the consensus reading, 23 lesions were rated as true-positive contrast-enhancing lesions and 11 as true-positive subacute bleedings. When compared with consensus reading, three false-negative and four false-positive lesions were noted on individual interpretations. Reader one missed a small parietally located lesion on the T1-weighted SE images, whereas reader two missed two small contrast-enhancing lesions on the MP RAGE images, one located in the choroidal plexus of the fourth ventricle and the other in the cortex of the temporal lobe. The four false-positive lesions recorded by one of the two readers were as follows: 1) On T1-weighted SE images, a prominent cortical vessel was read as a dotlike hyperintense lesion in the parietal cortex; 2) in another case on T1-weighted SE images, the combination of a prominent choroid plexus of the fourth ventricle and a pulsation artifact from the venous sinuses was read as a lesion (Fig 2); and 3) on MP RAGE images and 4) on VIBE images, a small vessel was read as a dotlike enhancing area in the basal ganglia in the same patient.

Ranks for lesion conspicuity assessed by the two readers in a side-by-side analysis are given in Table 3. Both readers rated T1-weighted SE highest for lesion conspicuity, followed by VIBE and then MP RAGE (Fig 3). For reader one, the conspicuity of lesions was significantly greater on T1-weighted SE images than on MP RAGE images ($P < .001$ for all hyperintense lesions, and $P = .02$ for contrast-enhancing lesions), but no statistically significant differences between T1-weighted SE images and VIBE images were found. On VIBE images, the conspicuity of all hyperintense

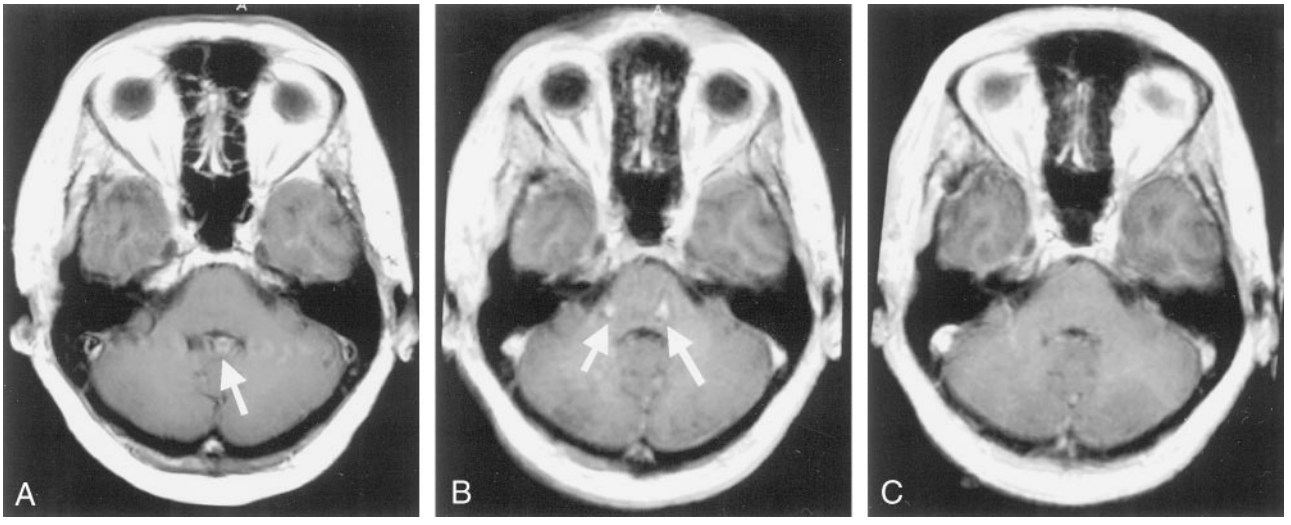

FIG 2. Images of the posterior fossa in a patient with suspected metastatic disease.
A, Two-dimensional T1-weighted SE image shows marked pulsation artifacts. Superimposition of the choroidal plexus in the fourth ventricle and the artifacts mimic a possible contrast-enhancing lesion (arrow).
B, MP RAGE 5-mm reformation shows considerable ghost artifacts (arrows) impairing visualization of the pons and the cerebellum.
C, VIBE 5-mm reformation shows no artifact.

TABLE 3: Lesion Conspicuity by Imaging Technique

Conspicuity Level and Lesion Type	T1-Weighted SE	VIBE	MP RAGE
Best*			
Contrast-enhancing	12.5 (14/11)	8 (8/8)	2.5 (1/4)
All hyperintense	20.5 (23/18)	10 (9/11)	3.5 (2/5)
Intermediate*			
Contrast-enhancing	4 (5/3)	9 (10/8)	10 (8/12)
All hyperintense	4.5 (5/4)	15 (18/12)	14.5 (11/18)
Lowest*			
Contrast-enhancing	6.5 (4/9)	6 (5/7)	10.5 (14/7)
All hyperintense	9 (6/12)	9 (7/11)	16 (21/11)
Average rank†			
Contrast-enhancing	1.7 (1.6/1.9)	1.9 (1.9/2.0)	2.4 (2.4/2.4)
All hyperintense	1.6 (1.6/1.9)	2.0 (1.9/2.0)	2.4 (2.6/2.2)

Note.—There were 34 hyperintense lesions of which 23 were contrast enhancing. Numbers in parentheses are separate results for the two readers.

* Data are the average number of lesions.

† Data are the average rank based on the ranking scheme 1 (best), 2 (intermediate), and 3 (worst).

lesions was rated significantly greater than that on MP RAGE images ($P = .003$), but this difference did not quite reach statistical significance for contrast-enhancing lesions ($P = .09$). Although a similar trend was observed, no statistical significance was found in the conspicuity ratings of the second reader ($P > .05$ for all comparisons). No statistical analysis was performed on the average ratings of the two observers because the interobserver concordance was low (in all cases, $\kappa < 0.27$).

Discussion

The major advantage of 3D imaging is the ability to acquire data with approximately isotropic resolution. This allows multiplanar reformatting, which simplifies imaging protocols and reduces measurement time when imaging in multiple planes is required. These advantages have been demonstrated in numerous studies (eg, 13). Although, in principle, isotropic resolution can be achieved with 2D sequences, this requires long RF pulse lengths that increase imaging time (14). Furthermore, narrow sections are often unavailable with 2D sequences, particularly on older systems. MP RAGE is a 3D sequence that allows the acquisition of 3D data sets in a reasonable time frame, while providing excellent GM-WM contrast (15). Our study shows that high-spatial-resolution T1-weighted 3D data sets of the brain can also be effectively obtained with VIBE. This technique, when configured to require the same imaging time as MP RAGE, demonstrates similar or slightly better contrast characteristics and fewer artifacts. Although both techniques use spoiled GRE sequences with ultrashort TRs and both are T1-weighted methods, the contrast mechanisms differ. With MP RAGE, contrast is developed by applying a nonselective 180° inversion pulse before rapid GRE acquisition. The contrast characteristics of this sequence depend on, among other parameters, the effective TI and on the length of the magnetization recovery period. With VIBE, contrast is developed in the same way as that of traditional GRE sequences and depends on TR and, more important, flip angle.

With VIBE, increased imaging efficiency is achieved by asymmetric k-space sampling and zero-filling in the section-select direction. Zero-filling is a method of interpolation that has become an established way to reduce partial-volume artifacts in 3D MR angiography (16). In combination with asymmetric sampling, zero-filling gives improved spatial resolution. The relationship between sampling asymmetry and spatial resolution is complex (17). However, when 108 asymmetrically sampled partitions are in-

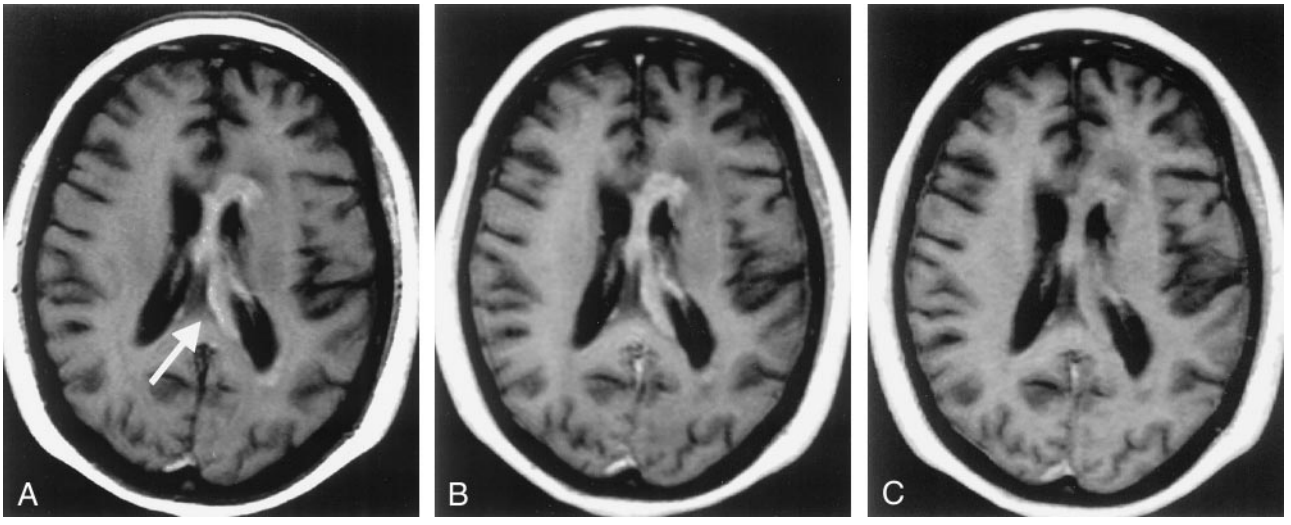

FIG 3. Primary cerebral lymphoma.
A–C, Interhemispheric contrast-enhancing lesion (arrow in *A*) is well visualized on both the 2D T1-weighted SE image (*A*) and the VIBE 5-mm reformation (*B*), but is less obvious on the MP RAGE 5-mm reformation (*C*).

terpolated to 216 (as was the case here), the partition resolution is greater than that which would be obtained with 108 symmetrically sampled partitions, but without the corresponding time penalty.

VIBE is an efficient sequence in that data samples are acquired continuously during the imaging period. With MP RAGE, approximately half of the acquisition time is required for magnetization preparation and recovery, during which no data are acquired. Thus, two signals could be obtained and averaged with VIBE in the time for acquisition using MP RAGE. This explains, at least partly, why SNR and CNR on VIBE images are better than those on MP RAGE images. Conversely, VIBE imaging times can be decreased or the sampling matrix can be increased without increasing imaging time by foregoing averaging, although these changes would be at the expense of SNR and CNR.

The VIBE sequence we used differs from that designed for gadolinium-enhanced MR angiography in two ways. First, the asymmetric echo in the read direction was replaced with a symmetric echo, which produces rather sharper images with less ringing artifacts (9). Second, the flip angle was chosen to give optimal CNR between GM and WM.

In phantom measurements, we found that VIBE offered better SNRs than did MP RAGE for T1 relaxation times that were shorter then 600 ms, which is a little below the T1 value for cerebral white matter (ie, 800 ms) (18). More important, the phantom results showed that the slope of the curve was steeper for VIBE than for MP RAGE, implying that contrast should be greater for contrast-enhancing lesions (Fig 1). This was borne out by the results of the patient study. The slopes of the GRE curves were also greater than the slope of the SE curve. However, overall, SE SNR was greater than that of either GRE sequence. These observations are consistent with our finding in patients that SE CNR was greater than that of either GRE sequence. Only at very short T1 values ($<$200 ms) did the GRE sequences give higher SNRs than that of the SE sequence owing to T2 effects and the longer TE of the SE sequence. This is in good agreement with the theoretic simulations of Mugler and Brookeman (5).

These short T1 values, however, do not seem likely to occur in contrast-enhancing lesions (19). A study comparing VIBE and SE imaging for lesion detection with use of a triple-dose of contrast agent might, however, be of interest and remains to be investigated. In previous studies (4,8), as well as in our study, contrast-enhanced lesions were missed on MP RAGE images, or seen with less conspicuity than on SE images. This can be explained by the favorable signal characteristics of SE images as determined by the phantom measurements and supported our findings of higher enhancing-lesion CNRs on SE images than on MP RAGE images. Similarly, our finding of superior lesion detection and lesion conspicuity on VIBE images compared with that on MP RAGE images might be attributed to the better CNR characteristics of VIBE. However, when lesion conspicuity was compared subjectively for the three imaging techniques, for most lesions differences in conspicuity were not considered large, and often readers did not agree on the ranking.

Acquisition time for the T1-weighted SE sequence was only half that of the GRE sequences. Doubling the number of averages for the SE sequence to give equal imaging times would improve both SNR and CNR by a factor of $\sqrt{2}$. However, in clinical practice, usually postcontrast T1-weighted images must be acquired in more then one plane. At least two separate acquisitions are therefore required for the SE T1-weighted sequence, but only one is necessary for VIBE and MP RAGE sequences. For cases in which only one plane is required, signal averaging would improve SE SNR and CNR commensurately. Equally, when three planes are required, SE SNR and CNR

would suffer relative to those of the GRE sequences when normalized for acquisition time.

There are recognized limitations in our comparison of lesion detection and conspicuity. First, we qualitatively compared only 5-mm VIBE and MP RAGE reformations. Comparing the 5-mm GRE reformations with the corresponding source images, we found, as expected, lower SNRs and CNRs for the source images. However, a smaller section thickness can be advantageous for the detection of small enhancing lesions in the brain, as partial volume effects are reduced (12). In our study, differences in SNR and CNR between the GRE sequences were more marked on the source images than on the 5-mm reformations. A study comparing the detection rate and conspicuity of enhancing lesions on VIBE and on MP RAGE source images may therefore be of value. However, this approach could not have been blinded because the different number of partitions (128 for MP RAGE versus 216 for VIBE) would have revealed the sequence. A second limitation was the limited number of small contrast-enhancing lesions in this study. We believe that the high interobserver variability for subjective ranking of lesion conspicuity was observed because most lesions were large and obvious on all images. A much larger number of patients and lesions would be required to determine differences in subjective ratings with statistical confidence.

Besides contrast-enhancing lesions, primary hyperintense lesions, which represented areas of subacute bleeding in all cases, were also assessed in a blinded fashion. All 11 subacute bleedings as seen on SE images were also depicted with high signal intensity on the GRE images. The high-signal-intensity display of the lesions with both GRE techniques is presumably due to the ultrashort TE used, which should be taken into account for correct image interpretation.

The reduced number of flow-related artifacts seen with both GRE sequences compared with the SE sequence is clearly advantageous, although the SE sequence did not include flow compensation gradients (20). We saw more flow artifacts with MP RAGE than with VIBE, possibly due to the use of signal averaging with VIBE only. These artifacts, either image blurring or discrete ghosts, severely impaired evaluation of posterior fossa structures, especially the pons, in some cases. SE images showed significantly fewer truncation artifacts, compared with both 3D GRE sequences. The appearance of these artifacts, caused by failure to sample high spatial frequencies, can be reduced by increasing the number of phase-encoding steps. The level of truncation artifacts was similar on VIBE and MP RAGE images, despite the smaller number of partitions in the former. This is presumably due to asymmetric sampling and interpolation to improve spatial resolution.

We used the manufacturer's recommended sequence parameters for MP RAGE. Although we have found that these yield good clinical images, it may be possible to optimize MP RAGE further. Technical enhancements such as alternative k-space ordering schemes have been reported, although, unlike the VIBE sequence, these are not commercially available (21). Moreover, asymmetric sampling and interpolation could be incorporated into MP RAGE to give a sequence combining the benefits of both; these modifications warrant further investigation.

Conclusion

Our results show that VIBE imaging provides an effective, alternative approach to MP RAGE imaging for 3D T1-weighted imaging of the brain. However, because of their lower CNRs, the GRE sequences in their current forms cannot replace the conventional T1-weighted SE sequence for lesion detection.

Acknowledgment

We thank Xiaonan Xue, PhD, Division of Epidemiology and Biostatistics, for help with statistical analysis.

References

1. Frahm J, Haase A, Matthaei D. **Rapid three-dimensional MR imaging using the FLASH technique.** *J Comput Assist Tomogr* 1986;10:363–368
2. Runge VM, Wood ML, Kaufman DM, Nelson KL, Traill MR. **FLASH: clinical three-dimensional magnetic resonance imaging.** *RadioGraphics* 1988;8:947–965
3. Mugler JP 3d, Brookeman JR. **Rapid three-dimensional T1-weighted MR imaging with the MP-RAGE sequence.** *J Magn Reson Imaging* 1991;1:561–567
4. Brant-Zawadzki M, Gillan GD, Nitz WR. **MP RAGE: a three-dimensional, T1-weighted, gradient-echo sequence—initial experience in the brain.** *Radiology* 1992;182:769–775
5. Mugler JP 3d, Brookeman JR. **Theoretical analysis of gadopentetate dimeglumine enhancement in T1-weighted imaging of the brain: comparison of two-dimensional spin-echo and three-dimensional gradient-echo sequences.** *J Magn Reson Imaging* 1993;3:761–769
6. van den Hauwe L, Parizel PM, Van Goethem JW, De Schepper AM. **Clinical usefulness of contrast-enhanced MP-RAGE of the brain.** *Neuroradiology* 1996;38(suppl 1):S14–19
7. Bluml S, Schad LR, Scharf J, Wenz F, Knopp MV, Lorenz WJ. **A comparison of magnetization prepared 3D gradient-echo (MP-RAGE) sequences for imaging of intracranial lesions.** *Magn Reson Imaging* 1996;14:329–335
8. Wenz F, Hess T, Knopp MV, et al. **3D MPRAGE evaluation of lesions in the posterior cranial fossa.** *Magn Reson Imaging* 1994; 12:553–558
9. Rofsky NM, Lee VS, Laub G, et al. **Abdominal MR imaging with a volumetric interpolated breath-hold examination.** *Radiology* 1999; 212:876–884
10. Buxton RB, Edelman RR, Rosen BR, Wismer GL, Brady TJ. **Contrast in rapid MR imaging: T1- and T2-weighted imaging.** *J Comput Assist Tomogr* 1987;11:7–16
11. Brant-Zawadzki MN, Gillan GD, Atkinson DJ, Edalatpour N, Jensen M. **Three-dimensional MR imaging and display of intracranial disease: improvements with the MP-RAGE sequence and gadolinium.** *J Magn Reson Imaging* 1993;3:656–662
12. Filippi M, Yousry T, Horsfield MA, et al. **A high-resolution three-dimensional T1-weighted gradient echo sequence improves the detection of disease activity in multiple sclerosis.** *Ann Neurol* 1996; 40:901–907
13. Mirowitz SA. **Intracranial lesion enhancement with gadolinium: T1-weighted spin-echo versus three-dimensional Fourier transform gradient-echo MR imaging.** *Radiology* 1992;185:529–534
14. Johnson G, Wadghiri YZ, Turnbull DH. **2D multislice and 3D MRI sequences are often equally sensitive.** *Magn Reson Med* 1999;41: 824–828

15. Mugler JP 3d, Brookeman JR. **Three-dimensional magnetization-prepared rapid gradient-echo imaging (3D MP RAGE).** *Magn Reson Med* 1990;15:152–157
16. Du YP, Parker DL, Davis WL, Cao G. **Reduction of partial-volume artifacts with zero-filled interpolation in three-dimensional MR angiography.** *J Magn Reson Imaging* 1994;4:733–741
17. Hurst GC, Hua J, Simonetti OP, Duerk JL. **Signal-to-noise, resolution, and bias function analysis of asymmetric sampling with zero-padded magnitude FT reconstruction.** *Magn Reson Med* 1992; 27:247–269
18. Bottomley PA, Foster TH, Argersinger RE, Pfeifer LM. **A review of normal tissue hydrogen NMR relaxation times and relaxation mechanisms from 1–100 MHz: dependence on tissue type, NMR frequency, temperature, species, excision, and age.** *Med Phys* 1984; 11:425–448
19. Aronen HJ, Niemi P, Kwong KK, Pardo FS, Davis TL. **The effect of paramagnetic contrast media on T1 relaxation times in brain tumors.** *Acta Radiol* 1998;39:474–481
20. Pattany PM, Phillips JJ, Chiu LC, et al. **Motion artifact suppression technique (MAST) for MR imaging.** *J Comput Assist Tomogr* 1987; 11:369–377
21. Deichmann R, Good CD, Josephs O, Ashburner J, Turner R. **Optimization of 3-D MP-RAGE sequences for structural brain imaging.** *Neuroimage* 2000;12:112–127